ResearchGate

See discussions, stats, and author profiles for this publication at: https://www.researchgate.net/publication/239717617

An Electrochemical Study of the SAMs of 6Mercaptopurine (6MP) at Hg and Au(111) Electrodes in Alkaline Media

ARTICLE *in* LANGMUIR · MAY 2002

Impact Factor: 4.46 · DOI: 10.1021/la011152q

CITATIONS
24

READS
32

4 AUTHORS, INCLUDING:

Rafael Madueño
University of Cordoba (Spain)
24 PUBLICATIONS **541** CITATIONS
SEE PROFILE

Teresa Pineda
University of Cordoba (Spain)
41 PUBLICATIONS **325** CITATIONS
SEE PROFILE

Manuel Blázquez
University of Cordoba (Spain)
76 PUBLICATIONS **884** CITATIONS
SEE PROFILE

Available from: Rafael Madueño
Retrieved on: 02 February 2016

An Electrochemical Study of the SAMs of 6-Mercaptopurine (6MP) at Hg and Au(111) Electrodes in Alkaline Media

Rafael Madueño, Teresa Pineda, Jose M. Sevilla, and Manuel Blázquez*

Departamento de Química Física y Termodinámica Aplicada, Universidad de Córdoba, Campus de Rabanales, C-3, 14071 Córdoba, Spain

Received July 23, 2001. In Final Form: November 16, 2001

A study of the reductive desorption process of 6MP-coated Hg and Au(111) electrodes in alkaline media has been carried out by means of such electrochemical techniques as cyclic voltammetry, chronoamperometry, and capacity−potential curves. The cyclic voltammograms show a single reduction peak whose peak potentials are strongly dependent on the nature of the substrate, Hg and Au(111) in this study. The full widths at half-maximum (fwhm) for Hg and Au(111) electrodes respectively are 19 and 21 mV at a scan rate of 0.1 V/s. These values are generally indicative of the existence of strong lateral interactions between molecules.The chronoamperometric curves have been recorded by single potential step experiments from a potential where the monolayer is stable to different final values within the range of potential where the monolayer is being desorbed. The curve shapes resemble those of systems that follow nucleation and growth mechanisms in the formation or dissolution of two-dimensional layers. In fact, the curve analysis using the nucleation and growth model of etching centers which was carried out in this report is actually in agreement with a mechanism of this kind for the dissolution of the 6MP monolayer at Hg and Au(111) electrodes. This study compares the properties of the 6MP monolayer at the two substrates Hg and Au(111) as well as with other thiol derivative monolayers.

Introduction

Self-assembled monolayers (SAMs) of organosulfur compounds on metal surfaces comprise a wide field of potential applications due to their versatility in modifying surfaces in a controllable manner. These systems have been studied with increasing interest in recent years, most of the studies being concerned with layers of aliphatic thiols on gold.[1−3] Short-chain alkanethiols have been shown to form less-ordered molecular packing demonstrating the importance of the van der Waals interactions between the parallel chains in the molecular packing structure.[4] SAMs of aromatic thiols have attracted much attention due to their high conductivity[5,6] and various other properties.[7−20] Aromatic thiols are very interesting molecules because they are highly anisotropic and thus enable intermolecular interactions to be stronger than those between *n*-alkanethiols. The reduced molecular flexibility of the rings and the $\pi \rightarrow \pi$ stacking interactions between aromatic molecules lead to molecular packing structures and ordering different from those commonly observed for alkanethiols. Moreover, a correlation is found between adsorption kinetics and the molecular dipole moment along the molecular axis[19] and with the dielectric constant of the solvent.[20]

The electrochemical properties of SAMs derived from aliphatic chains have been extensively studied focusing on the reductive desorption process at polycrystalline and single-crystal gold and silver[21−32] and Hg electrodes.[33−36] More recently, the removal of the monolayer has also been

* To whom correspondence should be addressed. E-mail: mblazquez@uco.es. Tel.: 34-957 21 86 46. Fax: 34-957 21 86 18.

(1) Ulman, A. *An Introduction to Ultrathin Organic Films From Langmuir-Blodgett to Self-Assembly*; Academic Press: New York, 1991.
(2) Finklea, H. O. In *Electroanalytical Chemistry*; Bard, A. J., Rubinstein, I., Eds.; Marcel Dekker: New York, 1996; Vol. 19, p 110.
(3) Schreiber, F. *Prog. Surf. Sci.* **2000**, *65*, 151.
(4) Ulman, A. *Chem. Rev.* **1996**, *96*, 1533.
(5) Dhirani, A.; Zehner, R. W.; Hsung, R. P.; Guyot-Sionnest, P.; Sita, L. R. *J. Am. Chem. Soc.* **1996**, *118*, 3319.
(6) Sachs, S. B.; Dudek, S. P.; Hsung, R. P.; Sita, L. R.; Smaley, J. F.; Newton, M. D.; Feldberg, S. W.; Chidsey, C. E. D. *J. Am. Chem. Soc.* **1997**, *119*, 10563.
(7) Ulman, A.; Kang, J. F.; Shnidman, Y.; Liao, S.; Jordan, R.; Choi, G.; Zaccaro, J.; Myerson, A. S.; Rafailovich, M.; Sokolov, J.; Fleischer, C. *Rev. Mol. Biotechnol.* **2000**, *74*, 175.
(8) Sabatini, E.; Cohen-Boulakia, J.; Bruening, M.; Rubinstein, I. *Langmuir* **1993**, *9*, 2974.
(9) Tao, Y.-T.; Wu, C.-C.; Eu, J.-Y.; Lin, W.-L.; Wu, K.-C.; Chen, C. *Langmuir* **1997**, *13*, 4018.
(10) Kolega, R. R.; Schlenoff, J. B. *Langmuir* **1998**, *14*, 5469.
(11) Jin, Q.; Rodriguez, J. A.; Li, C. Z.; Darici, Y.; Tao, N. J. *Surf. Sci.* **1999**, *425*, 101.
(12) Yoshimoto, S.; Yoshida, M.; Kobayashi, S.; Nozute, S.; Miyawaki, T.; Hashimoto, Y.; Taniguchi, I. *J. Electroanal. Chem.* **1999**, *473*, 85.
(13) Sawaguchi, T.; Mizutani, F.; Yoshimoto, S.; Taniguchi, I. *Electrochim. Acta* **2000**, *45*, 2861.
(14) Sato, Y.; Mizutani, F. *J. Electroanal. Chem.* **1999**, *473*, 99.
(15) Pineda, P.; Sevilla, J. M.; Román, A. J.; Blázquez, M. *Biochim. Biophys. Acta* **1997**, *1343*, 227.
(16) Sevilla, J. M.; Pineda, T.; Madueño, R.; Román, A. J.; Blázquez, M. *J. Electroanal. Chem.* **1998**, *442*, 107.
(17) Sevilla, J. M.; Pineda, T.; Román, A. J.; Madueño, R.; Blázquez, M. *J. Electroanal. Chem.* **1998**, *451*, 89.
(18) Madueño, R.; Sevilla, J. M.; Pineda, T.; Román, A. J.; Blazquez, M. *J. Electroanal. Chem.* **2001**, *506*, 92.
(19) Liao, S.; Shnidman, Y.; Ulman, A. *J. Am. Chem. Soc.* **2000**, *122*, 3688.
(20) Kang, J. F.; Liao, S.; Jordan, R.; Ulman, A. *J. Am. Chem. Soc.* **1998**, *120*, 9662.
(21) Widrig, C. A.; Chung, C.; Porter, M. D. *J. Electroanal. Chem.* **1991**, *101*, 335.
(22) Walczak, M. M.; Chung, C.; Stole, S. M.; Widrig, C. A.; Porter, M. D. *J. Am. Chem. Soc.* **1991**, *113*, 2370.
(23) Weisshaar, D. E.; Lamp, B. D.; Porter, M. D. *J. Am. Chem. Soc.* **1992**, *114*, 5860.
(24) Walczak, M. M.; Popenoe, D. D.; Deinhammer, R. S.; Lamp, B. D.; Chung, C.; Porter, M. D. *Langmuir* **1991**, *7*, 2687.
(25) Zhong, C.-J.; Porter, M. D. *Anal. Chem.* **1995**, *67*, 709.
(26) (a) Zhong, C.-J.; Zak, J.; Porter, M. D. *J. Electroanal. Chem.* **1997**, *421*, 9. (b) Wong, S.-J.; Porter, M. D. *J. Electroanal. Chem.* **2000**, *485*, 135
(27) Yang, D.-F.; Wilde, C. P.; Morin, M. *Langmuir* **1996**, *12*, 6570.
(28) Yang, D.-F.; Wilde, C. P.; Morin, M. *Langmuir* **1997**, *13*, 243.
(29) Yang, D.-F.; Al-Maznai, H.; Morin, M. *J. Phys. Chem.* **1997**, *101*, 1158.
(30) Mohtat, N.; Byloos, M.; Soucy, M.; Morin, S.; Morin, M. *J. Electroanal. Chem.* **2000**, *484*, 120.

10.1021/la011152q CCC: $22.00 © 2002 American Chemical Society
Published on Web 04/10/2002

Chart 1

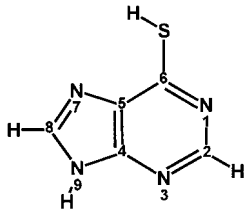

investigated by chronoamperometry.[37−41] The current transients have been analyzed by the nucleation and growth model in which the reductive removal of a thiol monolayer is initiated by the creation of etching centers and continues with the reduction of the thiols at the edge of the etching centers. However, to our knowledge, no paper has been published describing the analysis of an aromatic SAM by the chronoamperometric method.

This study deals with the electrochemical characterization of a SAM derived from 6-mercaptopurine (6MP) (Chart 1) at Hg and Au(111) electrodes in alkaline media. The study has been carried out through cyclic voltammetry, differential capacity, and chronoamperometric measurements. The monolayers formed at the two different substrates are compared.

Experimental Section

Chemicals. The 6MP was purchased from Sigma. All other reagents used were of Merck pa grade and were used without further purification.

As the supporting electrolyte, solutions of 0.1 M semiconductor-grade-purity potassium hydroxide (Aldrich) were used. Milli-Q purified water was used throughout to prepare solutions. Pure nitrogen was used to deaerate the working solutions.

Electrodes and Instrumentation. All electrochemical measurements were performed at a temperature of 25 ± 0.1 °C using thermostated Metrohm cells in a nitrogen atmosphere. The cell was enclosed in a grounded Faraday cage. Measurements were performed using a three-electrode cell comprising a Metrohm 50 mM KCl calomel electrode as reference electrode, a platinum wire as counter electrode, and a Hg or a gold single-crystal Au(111) as working electrode.

The Hg electrode was a Metrohm EA 290 hanging mercury drop electrode (HMDE) with an effective area of 0.0139 cm^2.

The Au(111) single-crystal electrode was 3 mm diameter and 2 mm thick cylinder from Crystal Oxide, with a polished side. A gold wire, mounted at its far tip, allowed easier handling of the crystal. Before each electrochemical measurement, the electrode was annealed in a small Bunsen burner flame to light red melt for about 20 s and, after a short period of cooling in air, quenched in ultrapure water. The electrode was then transferred into the electrochemical cell with a droplet of water adhering to it to prevent contamination. The surface condition was confirmed by a cyclic voltammogram in 0.01 M $HClO_4$, and the real surface area was determined from the reduction peak of oxygen adsorption on the Au electrode. This surface treatment was the most appropriate to produce a surface that is clean, ordered, and highly reproducible.

Voltammetric, chronoamperometric, and $C-E$ curves were recorded on an Autolab (Ecochemie model Pgstat20) instrument attached to a PC computer with proper software (GPES and FRA) for total control of the experiments and data acquisition. For the $C-E$ measurements, the amplitude of the sinusoidal signal at a frequency of 1 kHz was 10 mV.

For electrode modification, the freshly annealed Au(111) substrate or Hg drop were immersed in a 6MP solution (100 μM in 0.01 M $HClO_4$ to avoid sulfide contamination) during a fixed period of time. "Ex situ" experiments were performed with a modified surface as described above, after extensive washing with water or blank electrolyte and then transferred into the electrochemical cell. "In situ" electrochemical measurements were carried out in the presence of the modifier in solution.

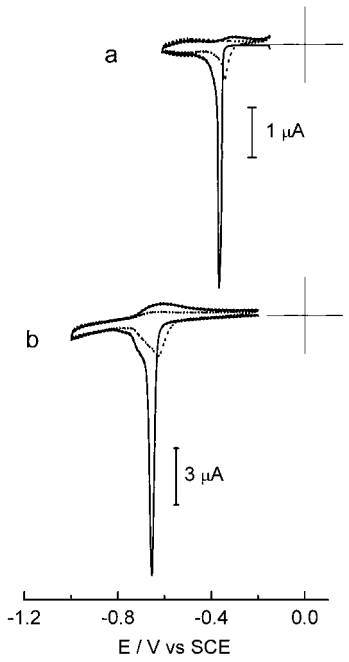

Figure 1. Consecutive cyclic voltammograms of 6MP-coated Hg (a) and Au(111) (b) electrodes in 0.1 M KOH at a potential scan rate of 100 mV/s: (−−) first cycle; (···) second cycle.

Results

The reductive desorption process undergone by spontaneously adsorbed 6-mercaptopurine (6MP) on Hg and Au(111) electrodes has been studied by means of cyclic voltammetry, capacity−potential curves and chronoamperometry.

Figure 1 displays two successive cyclic voltammograms of the 6MP-coated Hg and Au(111) electrodes from −0.15 to −0.6 V and from −0.2 to −1.0 V, respectively, in 0.1 M KOH. The coated electrodes are first immersed in the electrolyte solution at the initial potential and scanned in the negative direction. The only feature seen is a sharp reductive current peak at −0.37 and −0.65 V on Hg and Au(111), respectively. The small shoulder observed on the negative side of the desorption peak, which is clearer in the case of the Au electrode, could be due to desorption of a small fraction of chemisorbed molecules forming distinct phase domains.[18,26,30] When the potential is reversed and scanned in the positive direction, no oxidative features are observed. That single peak has been assigned to the reductive desorption process[21−30] represented by

$$\mathrm{Me-S-R} + 1e^- \rightarrow \mathrm{Me} + \mathrm{R-S}^- \qquad (1)$$

where Me stands for Hg or Au. On the second cathodic

(31) Hatchett, D. W.; Stevenson, K. J.; Lacy, W. B.; Harris, J. M.; White, H. S. *J. Am. Chem. Soc.* **1997**, *119*, 6596.
(32) Hatchett, D. W.; Uibel, R. H.; Stevenson, K. J.; Harris, J. M.; White, H. S. *J. Am. Chem. Soc.* **1998**, *120*, 1062.
(33) Stevenson, K. J.; Mitchell, M.; White, H. S. *J. Phys. Chem. B* **1998**, *102*, 1235.
(34) Demoz, A.; Harrison, J. D. *Langmuir* **1993**, *9*, 1046.
(35) Muskal, N.; Turyan, I.; Mandler, D. *J. Electroanal. Chem.* **1996**, *409*, 131.
(36) Muskal, N.; Mandler, D. *Electrochim. Acta* **1999**, *45*, 537.
(37) Calvente, J. J.; Kovácová, Z.; Sánchez, M. D.; Andreu, R.; Fawcett, W. R. *Langmuir* **1996**, *12*, 5696.
(38) Yang, D. F.; Morin, M. *J. Electroanal. Chem.* **1997**, *429*, 1.
(39) Yang, D. F.; Morin, M. *J. Electroanal. Chem.* **1998**, *441*, 173.
(40) Vinokurov, I. A.; Morin, M.; Kankare, J. *J. Phys. Chem. B* **2000**, *104*, 5790.
(41) Vela, M. E.; Martin, H.; Vericat, C.; Andreasen, G.; Hernandez Creus, A.; Salvarezza, R. C. *J. Phys. Chem. B* **2000**, *104*, 11878.

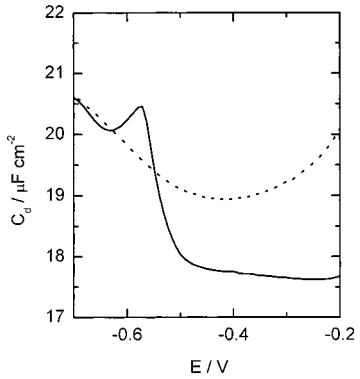

Figure 2. Capacitance−potential curves for a 6MP-coated Au(111) electrode in 0.1 M KOH. The dotted line represents the capacitance of the bare Au(111) electrode in the background electrolyte (0.1 M KOH).

(i.e. negative going) potential scan a minor peak displaced to positive potentials ($\Delta E \cong 20-30$ mV) is observed in both Hg and Au(111) electrodes. These peaks are ascribed to desorption of the 6MP molecules readsorbed during the first anodic scan. That positive potential shift has been explained as an indication that the readsorbed 6MP are desorbed more easily than the spontaneously adsorbed 6MP, as a consequence of the shift of the pzc and changes in the microenvironment at these lower coverages.[37]

The use of cyclic voltammetry to test the reduction of thiols on metallic electrodes has shown that such measurements provide quantitative values of surface concentration and qualitative information on the strength of the metal−sulfur bond.[21−41]

The value of the charge measured for 6MP desorption for Au(111) (54 μC/cm^2) is close to that reported in the literature for the reduction of other aromatic thiolate monolayers.[12−14] Assuming the one-electron reductive process given in eq 1, the coverage of 6MP is calculated to be 0.24 ($\Gamma = 0.56$ nmol/cm^2) (where the coverage of one monolayer corresponds to the density of atoms at the ideal 1×1 Au(111) surface equal to 1.39×10^{15} atoms/cm^2), equivalent to an average area of 29 Å^2/molecule.

In contrast, the charge value measured for 6MP desorption for Hg (71.3 μC/cm^2) is greater and corresponds to a coverage of 0.74 nmol/cm^2. Therefore, an average area of 22 Å^2/6MP molecule is found under these conditions. These results are similar to what has been reported for this system in acidic media[16] and reflect the formation of a denser monolayer in Hg than in Au(111).

On the other hand, the shapes of the desorption peaks for both Hg and Au(111) substrates are typical of highly packed monolayers. The full widths at half-maximum (fwhm), measured in the voltammograms obtained at 0.1 V/s as 19 and 21 mV for Hg and Au(111) electrodes, respectively, indicate strong lateral interactions between molecules.[42]

Additional information relative to the adsorption of 6MP on these substrates can be obtained by differential capacity measurements. Figure 2 shows $C-E$ curves for the bare- and 6MP-coated Au(111) electrode in 0.1 M KOH aqueous solution at 25 °C. The most striking feature found is the lower capacitance value observed at potentials positive to 6MP monolayer desorption as compared to the bare electrode. An important increase in capacitance occurs at the onset of desorption potential. A similar behavior is observed in the ex situ experiment carried out with the coated Hg electrode (Figure 3a). In both cases, the reverse scan shows a $C-E$ curve similar to the corresponding bare electrodes. It is interesting to note that when the experiments are undertaken "in situ", the reverse scans follow the same tendency as the direct ones, showing an important hysteresis between negative and positive scan directions (Figure 3b). This feature is typical of a kinetically controlled phase transition, in this case, from the condensed chemisorbed state to another whose specific characteristics are unknown at this moment.

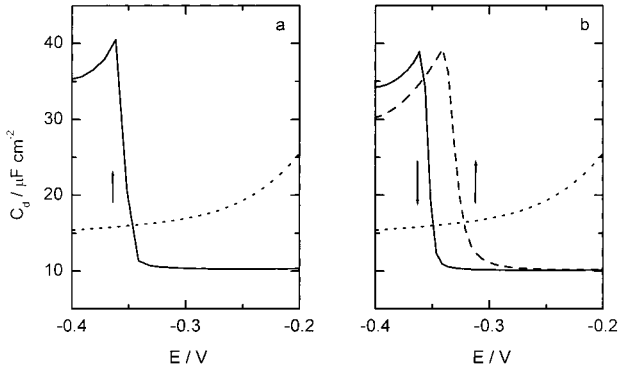

Figure 3. Capacitance−potential curves for a Hg electrode in 0.1 M KOH: (a) 6MP-coated electrode; (b) bare electrode in the presence of 100 μM 6MP. The arrows indicate the direction of the scan. The dotted line represents the capacitance of the bare Hg electrode in the background electrolyte (0.1 M KOH).

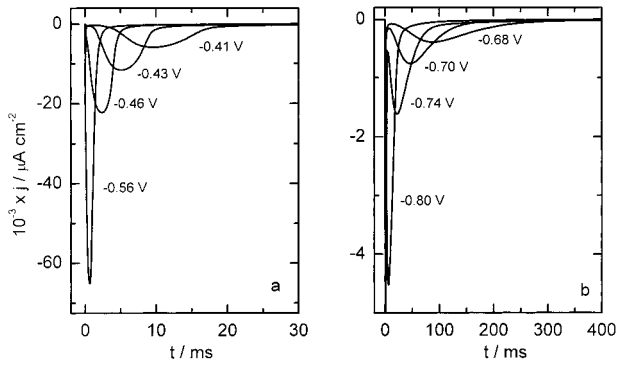

Figure 4. Current transients of 6MP-coated Hg (a) and Au(111) (b) electrodes, triggered by a single potential step. The magnitude of the final potential is indicated. Initial potentials (E_i) were −0.20 and −0.35 V for Hg and Au(111), respectively.

Dissolution kinetics in the 6MP chemisorbed layer are investigated by single potential step experiments carried out by selecting the initial potential at a value for which the layer is thermodynamically stable.

Figure 4a shows typical current−time curves obtained at 25 °C for the 6MP-coated Hg electrode in contact with a 0.1 M KOH aqueous solution after applying a single potential step from $E_1 = -0.2$ V to various final potentials at which 6MP desorption takes place. The chronoamperometric curves present an initial fast current transient peak associated with the charging of the double layer which is corrected by subtracting the chronoamperometric measurement made on the bare electrode for the same potential step. The charges of the current transients determined by the integration of the curve after the above-mentioned correction are equal (77 ± 6 μC/cm^2) for the different potential steps, and they are also close to that obtained in the cyclic voltammogram in Figure 1 (71.3 ± 4 μC/cm^2). The non-Faradaic contribution to the total reductive charge arising from the difference in capacitance between the electrode covered with the 6MP monolayer and the bare gold is ignored in this calculation given the small difference in capacitance values found in this system.

(42) Laviron, E. In *Electroanalytical Chemistry*; Bard, A. J., Ed.; Marcel Decker: New York, 1982; Vol. 12, p 53.

The chronoamperometric curve shape shows a strong dependency on the potential step (increases in current in a decade correspond approximately to 90 mV of increase in potential step). The presence of current maxima in the curves indicates that desorption kinetics involves the nucleation and growth of two-dimensional holes.

Figure 4b shows the chronoamperometric curves for the 6MP-coated Au(111) under the same conditions as described above for Hg. The initial potential for these curves is $E_1 = -0.35$ V. The chronoamperograms are found to be similar to those obtained for the Hg electrode. After correction of the charging current, the integrated charges of the current transients are slightly greater (66 ± 5 μC/cm^2) than those obtained from cyclic voltammetry in Figure 1 (54 ± 7 μC/cm^2). This difference was also found by Calvente et al.[37] in their study on the desorption of 2-mercaptoethanesulfonate on Au(111) and explained as being due to solvent reduction on the structurally modified gold surface. A careful examination of the curves in Figure 4b shows that the current does not fall to zero at longer times in all the potential steps.

Discussion

The reductive electrodesorption of SAMs has been used to study thiol−thiol interactions.[32,33,41] In fact, SAMs on Au(111) and Ag(111) are desorbed in sharp voltammetric current peaks whose peak potentials shift in the negative direction as the number of C atoms, n, increases in the alkanethiol molecules. On the basis of the shift of the peak potential E_p with n and assuming adsorption/desorption equilibrium, intermolecular forces acting at SAMs of thiols on Ag(111) and Hg have been estimated.[32,33] However, Vela et al.[41] have found that the value of $E_{p(v\to 0)}$ (determined by plotting E_p vs v and extrapolating for $v = 0$) extrapolated for $n = 0$ indicates that the S−Au bond energy in the thiol lattice is ≅19 kJ/mol smaller and that the bond has a lesser ionic character than the S−Au bond in a sulfur lattice. A similar finding has been described by Yoshimoto et al.[12] for the electrodesorption of pyridinethiol on Au(111). In fact, the desorption peak potential of pyridinethiol (−0.53 V vs Ag/ClAg, saturated KCl) was more positive by ca. 0.4 V than that of sulfide (−0.9 V) in an alkaline solution and adsorbed pyridinethiol was easily replaced by sulfide.

In the case of 6MP, behavior similar to that of pyridinethiol is observed. The potential of desorption of the 6MP in Au(111) is −0.65 V at 0.1 V/s. The value of $E_{p(v\to 0)}$ found is −0.525 V vs SCE. From this potential value, an adsorption energy of −26.7 kJ/mol has been obtained (after the values are converted to the NHE scale). On the other hand, the adsorption energy of 6MP on Hg is −7.4 kJ/mol, determined by using $E_{p(v\to 0)} = -0.325$ V as the value.

It does not make any sense to compare the adsorption free energy obtained on the basis of the potential of the reductive desorption of SAMS derived from alkanethiols to the energy given off by aromatic thiols. First, the values estimated for alkanethiols increases linearly with chain length, thus indicating an increase in lateral interactions. Second, the extrapolated value of ΔG_{ads} at $n = 0$ is interpreted as the free energy associated with the formation of the metal−S bond.[32] However, ΔG_{ads} obtained in this study for 6MP is lower than the values obtained for alkanethiols of short length. Therefore, the interpretation of these values needs to be different from that of alkanethiols. The desorption potential of aromatic thiols is less negative than that of alkanethiols.[9] However, in the case of the desorption of 6MP studied in this work, we found an important difference with respect to the other aromatic SAMs. This difference is the very sharp peaks obtained with a fwhm of 19 and 21 mV in Hg and Au(111), respectively. The theoretical value for a monoelectronic reversible reaction is 90.6 mV at 25 °C.[42] This fact is explained as being due to strong interactions between chains. In this case, the purine molecules are known to stack in aqueous solutions at low concentrations. So it is probable that the molecules bind to the gold surface in a stacked structure, and it is also possible that desorption takes place in a cooperative manner. On the other hand, the packing behavior observed for almost all the aromatic SAMs is the herringbone structure,[8] which is not the most probable for 6MP if we assume stacking interactions between rings in such a way that most of the ring area makes contact between molecules. The distance of maximum approach between two stacked purine rings is 3.5 Å;[43] from our data of surface area/molecule calculated from voltammetric results, the dimensions of the molecule adsorbed at Au(111) would be 3.5×8.3 Å^2. We can rule out the possibility of *face-on* adsorption for the 6MP molecule, on the basis of STM data of the adsorption of this molecule on Au(111)[44] and also from SERS,[45] where it is shown than 6MP adsorbs in different orientations but always *side-on*, over the Ag surface.

Chart 2

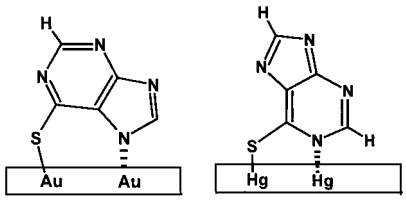

In the case of Hg, the area/molecule obtained from electrochemical data is lower than in Au(111). The difference could be explained on the basis of more compact packing of 6MP molecules; in fact, an excess of 6MP molecules of around 30% is adsorbed on Hg over Au(111). However, this difference can be explained if it is assumed that the molecules adsorb with a different orientation. It has been described how, when 6MP chemisorbs to a metal surface (either gold or silver), not only the sulfur atom but also the nitrogen atoms in the rings (either in position 7 or 1) (see Chart 1 for numbering) can interact with those surfaces. So, the interaction in gold probably takes place through the N7 causing the molecule to occupy a larger surface area while in Hg the interaction occurs through the N1, resulting in a lower surface area/molecule (Chart 2). A rough estimation of the projection area of the molecule over the surface, taking into account the crystallographic dimensions of the 6MP molecule[46,47] in these two configurations, agrees with the 30% difference in the surface excess of 6MP in Hg and in Au(111). The liquid nature of Hg may help the 6MP molecule to adopt this configuration which apparently creates a more compact monolayer, whereas the atomic arrangement of the Au(111) surface forces the 6MP molecule to adopt the other. This fact is in agreement with ESCA data obtained for 6MP adsorbed on Au(111), which indicate that one molecule adsorbs for approximately six gold atoms.[44]

(43) Cantor, C. R.; Schimel, P. R. *Biophysical Chemistry. Part I: The conformation of biological macromolecules*; W. H. Freeman and Co.: New York, 1980; p 328.
(44) Boland, T.; Ratner, B. D. *Langmuir* **1994**, *10*, 3845.
(45) Vivoni, A.; Chen, S.-P.; Ejeh, D.; Hosten, C. M. *Langmuir* **2000**, *16*, 3310.
(46) Sletten, E.; Sletten, J.; Jensen, L. H. *Acta Crystallogr.* **1969**, *B25*, 1330.
(47) Brown, G. M. *Acta Crystallogr.* **1969**, *B25*, 1338.

On the other hand, surface Au atoms in an aromatic thiol monolayer[11] have been reported to be much more mobile than the atoms on bare Au surfaces. This increased mobility occurs because the strong Au−S bond weakens the adhesion between the Au atoms within the top layer and between the top and second layers. The contribution from the $\pi-\pi$ stacking interactions, which are stronger than the van der Waals interactions of the alkanethiols SAMs, favors aggregations of the adsorbed aromatic molecules into islands. This process involves many gold atoms in a collective way, the final result of which should be a decrease in surface roughness allowing the ordered domains to increase. In fact, the time evolution includes the coalescence into bigger size islands or the incorporation of those nearby the step edges into them. Moreover, STM reveals that molecules pack into the same structure both on and between islands.[11] Therefore, it can be assumed that this phenomenom should no affect the value of surface area/molecule calculated from the charge density results for the Au(111) electrode.

An interesting feature in the curves in Figure 4 is the fact that the dissolution process (electrochemical desorption) is faster in Hg than in Au(111) even though the 6MP monolayer should be more compact at Hg. Thus, other factors must explain that difference in the desorption process kinetic of the two substrates.

The different role played by the substrate nature is an important point to take into account. If the metal pzc values are considered (+0.32 V vs SCE for Au(111)[48] and −0.44 V vs SCE for Hg[49]), then the dissolution of the 6MP monolayer results in a practically neutral surface in Hg whereas the surface is negatively charged in Au(111). A behavior of this type has been found in uracil chemisorption and its methyl derivatives[50] and uridine[51] on different substrates. The different ranges of potential where stable chemisorbed species exist are attributed to their interaction via an overlapping of nonbonding orbitals in the molecules and the d-bands in the metals. These d-bands are located at 8, 4, and 2 eV below the Fermi level for Hg, Ag, and Au, respectively. Thus, the overlapping of the orbitals is more favorable at Au than at Hg. On the other hand, it has been found[52] that the rate of hole nucleation is enhanced by the presence of defects in the film, while the radial hole growth is slowed by their presence. Thus, the liquid nature of Hg, with a defect-free surface, may create a more homogeneous monolayer and accelerate the desorption process which is faster than in Au(111), where the presence of defects cannot be ruled out.

The analysis of the chronoamperograms was carried out with models used in the literature for the study of the reduction mechanism of thiols chemisorbed on Au(111).[38,39] These models take into account known nucleation and growth processes used to describe the electrodeposition and dissolution of metals and nonmetal layers, organic monolayers, and charge transfer in polymer-coated electrodes.[48−51] In this case, the reductive removal of a thiol monolayer is initiated by the creation of etching centers (holes) and continues with the reduction of the thiols that are at the edge of the etching centers.

Two sets of conditions for the nucleation and growth model have been reported.[53,54,57−59] The first set occurs when a small overpotential is applied to the thiol-coated electrode, making the rate of creation of the etching centers similar to their rate of growth. This model is called progressive etching center creation and growth and could be analyzed by eq 2:

$$\frac{I}{I_m} = \frac{t^2}{t_m^{\,2}} \exp\left(\frac{-2(t^3 - t_m^{\,3})}{3t_m^{\,3}}\right) \qquad (2)$$

where I is the current at time t after the potential step and I_m is the maximum current which occurs at time t_m.

The other limiting case occurs for larger overpotentials when the rate of growth of the etching centers becomes larger than the rate of creation of the etching centers. This model is called instantaneous etching center creation and growth:

$$\frac{I}{I_m} = \frac{t}{t_m} \exp\left(\frac{-(t^2 - t_m^{\,2})}{2t_m^{\,2}}\right) \qquad (3)$$

The application of a large overpotential leads to desorption from a limited number of etching centers. When a more negative final potential is reached, the reductive removal occurs homogeneously across the electrode surface instead of only at a few etching centers. The asymmetric chronoamperograms obtained in this case are probably due to the increased rate of cation diffusion and solvent molecules throughout the organic monolayer. For very large overpotentials, the rate of growth of the etching centers becomes limited by the diffusion of the reduced thiols away from edge of the etching centers. Thus, the growth of the etching centers will be slow compared to their rate of creation. Consequently, the reductive current will arise mainly from the formation of etching centers. This model has been called homogeneous reduction process by Morin et al.,[38,39] and the normalized current can be expressed by the eq 4

$$\frac{I}{I_m} = \left(\frac{k_3}{k_n + k_3}\right)^{-k_3/kn} \cdot \frac{k_n + k_3}{k_n} [\exp(-k_3) - \exp(-(k_n + k_3)t)] \qquad (4)$$

In this equation k_n is the rate of creation of etching centers and k_3 is the rate of thiol reduction during the creation of an etching center.

With these models we have analyzed the chronoamperograms obtained by the reduction of the 6MP monolayer chemisorbed on Hg and Au(111) electrodes.

The results of the fitting of the chronoamperometric curves corresponding to Hg are shown in Figure 5. The overall shape of the transient current is well described by the progressive model for a potential step of −85 mV (this potential step refers to the difference between the final potential and $E_{p(v\to 0)}$). At a potential step of −135 mV, the reduction of the monolayer is between a progressive and an instantaneous etching process. With increase of the potential step ($\Delta E_p = -235$ mV) the overall transient

(48) Kolb, D. M. *Prog. Surf. Sci.* **1996**, *51*, 109.
(49) Grahame, D. C.; Coffin, E. M.; Cummings, J. I.; Poth, M. A. *J. Am. Chem. Soc.* **1952**, *74*, 1207.
(50) Wandlowski, T. *J. Electroanal. Chem.* **1995**, *395*, 83.
(51) Van krieken, M.; Buess-Herman, C. *Electrochim. Acta* **1999**, *45*, 675.
(52) Van krieken, M.; Buess-Herman, C. *Electrochim. Acta* **1998**, *43*, 2831.
(53) Harrison, J. A.; Thirsk, H. R. In *Electroanalytical Chemistry*; Bard, A. J., Ed.; Marcel Dekker: New York, 1971; Vol. 5, p 67.
(54) Schmickler, W. *Interfacial Electrochemistry*; Oxford University Press: Oxford, U.K., 1996; Chapter 10.
(55) Muller, C.; Albalat, R.; Gómez, E.; Sarret, M.; Valles, E. *Electrochim. Acta* **1989**, *34*, 781.
(56) Muller, C.; Claret, J.; Sarret, M. *J. Electroanal. Chem.* **1986**, *207*, 263.
(57) Avrami, M. *J. Chem. Phys.* **1937**, *7*, 1130.
(58) Avrami, M. *J. Chem. Phys.* **1940**, *8*, 212.
(59) Avrami, M. *J. Chem. Phys.* **1941**, *9*, 177.

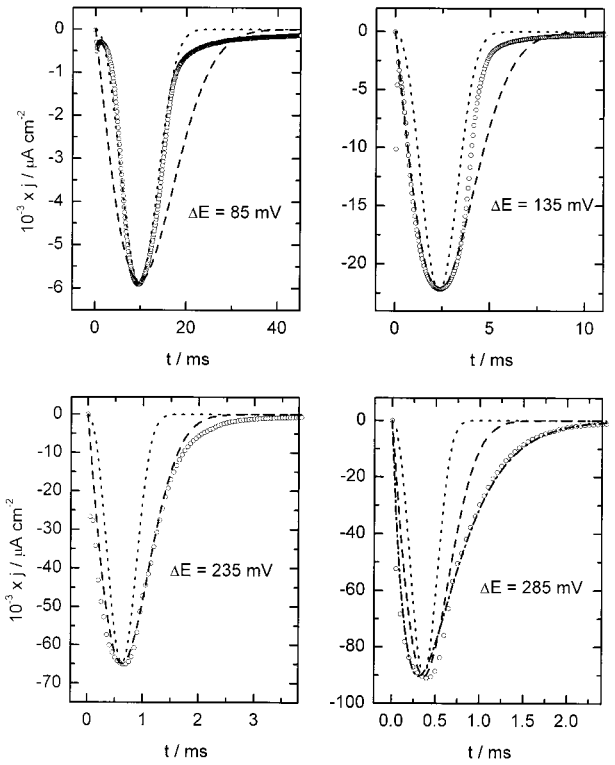

Figure 5. Current transients of 6MP-coated Hg electrode in 0.1 M KOH: (○○○) chronoamperometric data; (···) fit with the progressive etching center creation and growth model (eq 2); (− − −) fit with the instantaneous etching center creation and growth model (eq 3); (− · − · −) fit with the homogeneous reduction model (eq 4). The magnitude of the potential values (ΔE) is indicated and referred to the $E_{p(v\rightarrow 0)}$.

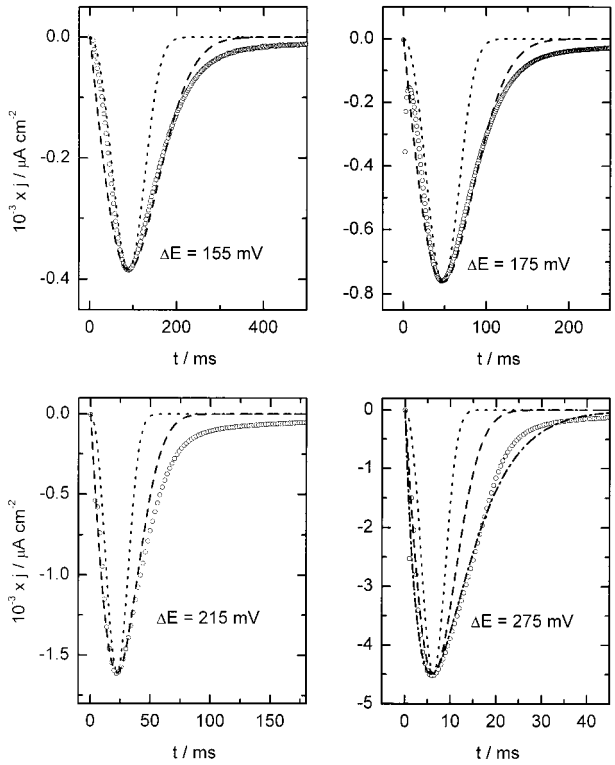

Figure 6. Current transients of 6MP-coated Au(111) electrode in 0.1 M KOH: (○○○) chronoamperometric data; (···) fit with the progressive etching center creation and growth model (eq 2); (− − −) fit with the instantaneous etching center creation and growth model (eq 3); (− · − · −) fit with the homogeneous reduction model (eq 4). The magnitude of the potential values (ΔE) is indicated and referred to the $E_{p(v\rightarrow 0)}$.

current is well described by an instantaneous etching process. Finally, in the case of potential steps to larger overpotentials (i.e., $\Delta E_p = -285$ mV), the etching center creation and growth model fails. The overall curve is well described by the homogeneous process (eq 4), where intermolecular interactions play an important role in diffusion control. This behavior is similar to that reported by Morin et al. for a nonanethiol monolayer on Au(111).[39] The high 6MP concentration that should be reached near the mercury surface and its low solubility due to intermolecular interactions make the growth of the etching centers more difficult, and this could lead to a homogeneous reduction in 6MP for larger overpotentials.

Figure 6 shows the fitting of the chronoamperograms corresponding to the 6MP reduction in Au(111). The behavior of this system is parallel to that just described for the Hg electrode. In no case does the transient current fall to zero. This is the same behavior observed in 2-mercaptoethanesulfonate on Au(111) by Calvente et al., where a concomitant non-Faradaic process is measured in chronoamperograms.[37]

It seems that the same mechanism is operative for the desorption of the 6MP monolayer on Hg and Au(111) electrodes. Moreover, it is also similar to the behavior observed in the desorption process of alkanethiol monolayers on gold. However, it is worth noting that the kinetics of the reduction process is very dependent on the nature of the substrates. Figure 7 represents the values of t_{max} (the time where the current density in the transients is maximum) as a function of the potential step ΔE_p, for Hg and Au(111) electrodes. An important difference in the time scale of the process is observed at small overpotentials, while convergence is found at the larger steps, in agreement with the fact that homogeneous reduction

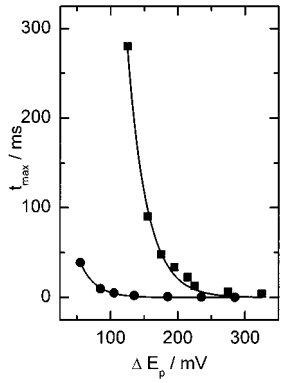

Figure 7. Influence of the nature of the electrode on the dissolution process expressed by t_{max} for the 6MP-coated (●) Hg and (■) Au(111) electrodes in 0.1 M KOH. Transitions triggered by a potential step from −0.2 V (for Hg) and −0.35 V (for Au(111)) to various final potentials are referred to $E_{p(v\rightarrow 0)}$.

should be independent of the substrate nature. Assuming that the rate of hole nucleation is higher at Au(111) than at Hg, given the absence of defects in the latter's surface, the growth of those holes needs to be much faster at Hg resulting in a slower global process at the Au(111) substrate.

In summary, the behavior of the 6MP molecule in its self-assembly process is found to be of great interest. An important fact is that the molecule can exist in several tautomeric forms with differences in stability not only in a noninteracting environment but also upon changing to an interacting environment. Contribution to these differences by the dipole moment magnitude has been reported on the basis of quantum-mechanical approaches.[60]

In this respect, the important dipole moment of the molecule needs to be taken into account when analyzing the stability of the 6MP monolayer. The above proposed different orientations of the molecule (Chart 2) in Hg and Au(111) gives dipole moment values along the vertical to the surface, which are also different, and as has been reported by Kang et al.,[20] the monolayer should be considered as a two-dimensional array of dipoles. Thus, the stabilization of that polar SAM through dipolar interactions with the polar solvent molecules arranged in the monolayer is another factor that has to be taken into account. The difference in the reductive desorption potential obtained for the 6MP monolayer at the two substrates used in this work should be related to the above-mentioned stabilization by water molecules near the monolayer.

Conclusions

The electrochemical techniques used in this work for the study of the reductive desorption process of 6MP-coated Hg and Au(111) electrodes in alkaline media give some insights into different aspects concerning the 6MP monolayer.

The sharp reduction peaks obtained by cyclic voltammetry of the 6MP SAMS have led us to conclude that strong interactions between rings might exist in both substrates. This is in contrast to the reduction potential which is less negative than those of short-length alkanethiols. On the basis of the literature results,[11] this is explained as a result of increased metal surface atom mobility in aromatic SAMS, due to stronger interactions between rings.

The chronoamperometic curves have been analyzed by using the hole nucleation and growth mechanism, and a good agreement has been found in the fitting of the theoretical equations to the experimental curves. Therefore, it can be said that the 6MP SAMS formed on Hg and Au(111) electrodes are desorbed by following a mechanism of this type.

The different data of surface area/molecule, determined by cyclic voltammetry and chronoamperometry (i.e., 22 and 29 $Å^2$/molecule at Hg and Au(111) surfaces, respectively) are interpreted as differences in the orientation of the molecule upon assembly. This latter feature is unique to this type of aromatic molecule with a heteroatomic two-ring structure, given the tautomeric equilibrium in which it is involved and, most importantly, the changes in the dipolar moment upon the adoption of different orientations. Studies regarding this latter issue are being undertaken in our laboratory.

Acknowledgment. This work is supported by a Grant for Scientific Research by the DGES (Project PB97-0469) from the Ministerio de Educación y Cultura of Spain, the Junta de Andalucia, and the University of Cordoba.

LA011152Q

(60) Lapinski, L.; Nowak, M. J.; Kwiatkowsci, J. S.; Leszczynski, J. *J. Phys. Chem. A* **1999**, *103*, 280.